

New Cancellation Technique for Electromagnetic Induction Sensors

Waymond R. Scott, Jr. and Michael Malluck
Georgia Institute of Technology
School of Electrical and Computer Engineering
Atlanta, GA 30332-0250

ABSTRACT

A new technique is presented for canceling the coupling between the coils of an electromagnetic induction sensor while using simple dipole detection coils. A secondary bucking transformer is used to cancel the coupling between the coils. The technique allows the cancellation that can be obtained using a quadrupole receive coil while maintaining the depth sensitivity and simple detection zone of a dipole coil. Simple circuit models for the sensor with some of the important parasitic effects are developed. An experimental model is developed and used to demonstrate the technique. Experimental results are presented that demonstrate more than 75 dB of cancellation up to 100 kHz and the response of the sensor to a few targets.

Keywords: Landmine Detection, EMI, Electromagnetic Induction, Metal Detector

Introduction

For many years, extensive effort has been expended developing techniques for locating land mines. For a mine detection technique to be successful there must sufficient contrast between the properties of the mine and the earth. There also must be sufficient contrast between the properties of the mine and common types of clutter such as rocks, roots, cans, etc. so that the mine can be distinguished from the clutter. The latter condition is the most problematic for most mine detection techniques. For example, simple electromagnetic induction (EMI) sensors are capable of detecting most mines; however, they will also detect every buried metal object such as bottle tops, nails, shrapnel, bullets, etc. This results in an unacceptable false alarm rate. This is even more problematic for low-metal anti-personnel mines as they are extremely difficult to distinguish from clutter using a simple EMI sensor. In recent years, advanced EMI sensors that use a broad range of frequencies or a broad range of measurement times along with advanced signal processing have been shown to be capable of discrimination between buried land mines and many types of buried metal clutter [1-4]. For these advanced EMI sensors to be effective, they must be able to accurately, repeatably, and quickly measure the response of a buried target. This is difficult because the sensor must operate with bandwidths greater than 100 to 1 while accurately measuring signals that are more than 80 dB smaller than the direct coupling between the coils on the EMI sensor. In order to accomplish this, the EMI sensor must be very cleverly designed to account for the coupling and for the secondary effects such as resonances in the coils.

In most EMI sensors, the coupling between the coils is handled by one of two methods. In time-domain sensors, the coupling between the coils can be mostly removed by time gating if the coils are properly designed. In frequency domain sensors, the coupling is mostly removed by using a quadrupole receive coil which minimizes the mutual inductance between the coils. The coils are usually formed using one of three common forms. In the first form, the receive coil is wound in a figure 8 pattern. In the second form, two receive coils of the same size and numbers of turns are wound on the same axis and are spaced a distance apart. The two coils are wound in opposite directions. In the third form, the coils are wound coaxially on the same plane and in opposite directions. In all of these forms, the coils are wound so they will have minimal coupling to the transmitting coil. All of these forms have the disadvantage of being less sensitive to deeply buried targets and having a complicated detection zone when compared to a dipole receive coil.

A new technique is presented for canceling the coupling between the induction coils while maintaining the depth sensitivity and simple detection zone of a dipole coil. Here simple dipole transmit and receive coils are used along with a secondary bucking transformer to cancel the coupling between the coils. A similar use of a bucking transformer was presented for a system operating below 1 kHz in a patent issued in 1972 [5], but the patent does not present a method for compensating for parasitic effects which is crucial at higher frequencies.

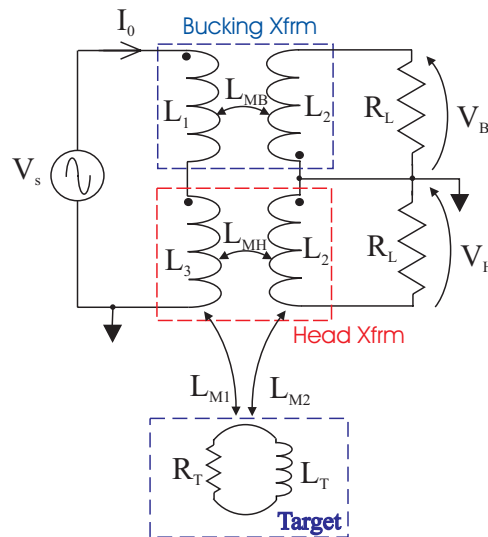


Figure 1. Basic configuration of the technique.

Approach

Figure 1 shows a basic diagram of the system where simple dipole transmit and receive coils are used along with a secondary transformer to cancel the direct coupling between the coils. Here the exciting current I_o passes through the primary coils of both the bucking and head transformers and induces a voltage in the secondary transformers. The voltage induced in the secondary windings of the head transformer depends on its mutual inductance as well as the coupling through the target:

$$V_H = j\omega L_{MH} I_0 - \frac{\omega^2 L_{M1} L_{M2}}{R_T + j\omega L_T} I_0.$$

The first term in the equation above is due to the direct coupling between the coils of the head transformer and is generally much larger than the second term which is due to the target. The voltage induced in the secondary windings of the bucking transformer depends only on its mutual inductance:

$$V_B = -j\omega L_{MB} I_0.$$

The response of the target is obtained from the relation

$$R = \frac{V_H + V_B}{V_B} = \frac{j\omega L_{M1} L_{M2}}{L_{MB} (R_T + j\omega L_T)}$$

if we make $L_{MH}=L_{MB}$. This is the ideal response (scaled by L_{MB} , L_{M1} , and L_{M2}) that we want to obtain with the direct coupling term eliminated. Unfortunately, it is difficult to exactly match the mutual inductances. In figure 3, a method for compensating for the mismatch of the mutual inductances is shown. It is a simple voltage divider that effectively allows us to match the inductances by simply tuning a resistive pot when $L_{MB} > L_{MH}$. In addition, the diagram in figure 1 is a good model at low frequencies (<1 kHz), but it omits several important parasitic elements at higher frequencies (>1 kHz).

A diagram with some of the important parasitic elements is presented in figure 2. These parasitic elements significantly reduce the effectiveness of the cancellation obtained above. One method of compensation for these parasitics is shown in figure 3. Here R_{Q1} and R_{Q2} are the series resistance of the secondary windings of the transformers, and C_{Q1} and C_{Q2} are the inter-winding capacitances of the windings plus the capacitance of the cable connected to the windings. These capacitances and resistances cause a resonance when added to the inductance of the windings.

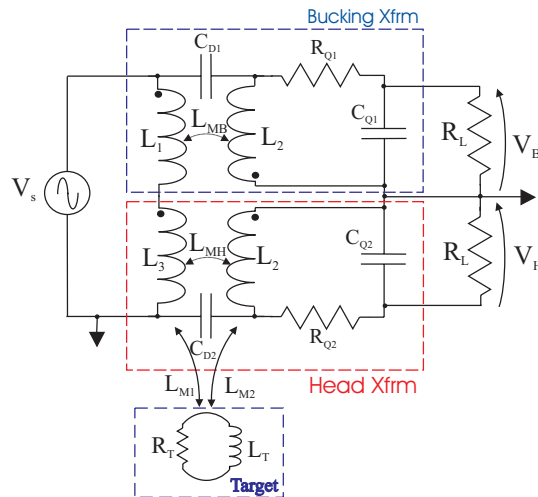


Figure 2. Diagram of EMI sensor with important parasitic elements.

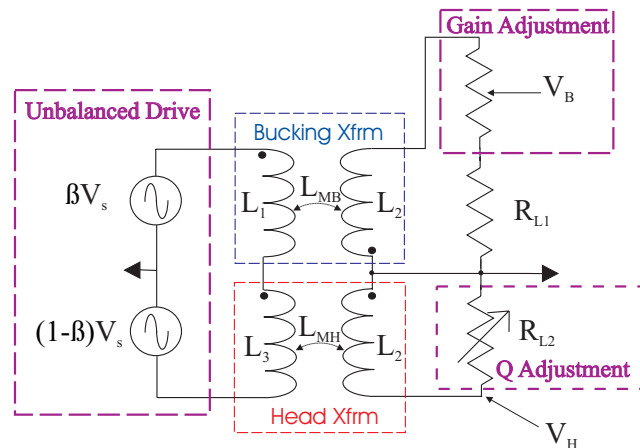


Figure 3. Diagram of EMI sensor with compensating elements.

Since it is impossible to eliminate these capacitances and resistances, the best we can do is to make the resulting resonances at frequencies much higher than the operating band of the sensor and to make the resonant frequency and Q for each of the secondary windings of the transformers as close to each other as possible. For the transformers that we have constructed so far, it has been sufficient to match the Q's of the coils by varying the load impedance imposed on the secondary windings of the transformers, as in figure 3. Here, R_{L2} is adjusted to match the Q's.

In figure 2, the capacitances C_{D1} and C_{D2} , model the effects of the capacitance between the primary and secondary windings of the transformer. These can be mostly eliminated by proper shielding of the transformers, but still may be problematic at higher frequencies. In figure 3, an unbalanced drive signal is used to compensate for these capacitances.

Experimental Model and Results

An experimental model for the sensor shown in figure 3 was constructed and used to demonstrate these ideas. In figure 4, photographs of the components used in the experimental model are shown. An Agilent model 4395A network analyzer was used to measure the transfer function of the system, and four Stanford Research systems SR560 amplifiers were used in the system. Two SR560s were used as differential preamplifiers to amplify the signals V_H and $V_B - V_H$ and two SR560s were used as power amplifiers for the unbalanced drive signal. These amplifiers were used for the drive as a matter of convenience in that they were readily available, but they can only drive approximately 100mA through the transformers which significantly limits the performance of the system. They will be replaced with stronger amplifiers in the future.

The head transformer was made from an FR4 circuit board with 2 oz copper cladding. The primary winding has 20 turns and a radius of 4.75 inches, and the secondary winding has 20 turns and a radius of 3 inch. The traces for the primary winding are 40 mils wide with 10 mil spacing, and the traces for the secondary winding are 20 mils wide with 10 mil spacing. The bucking transformer was made as a toroidal transformer to minimize its sensitivity to metal objects placed in

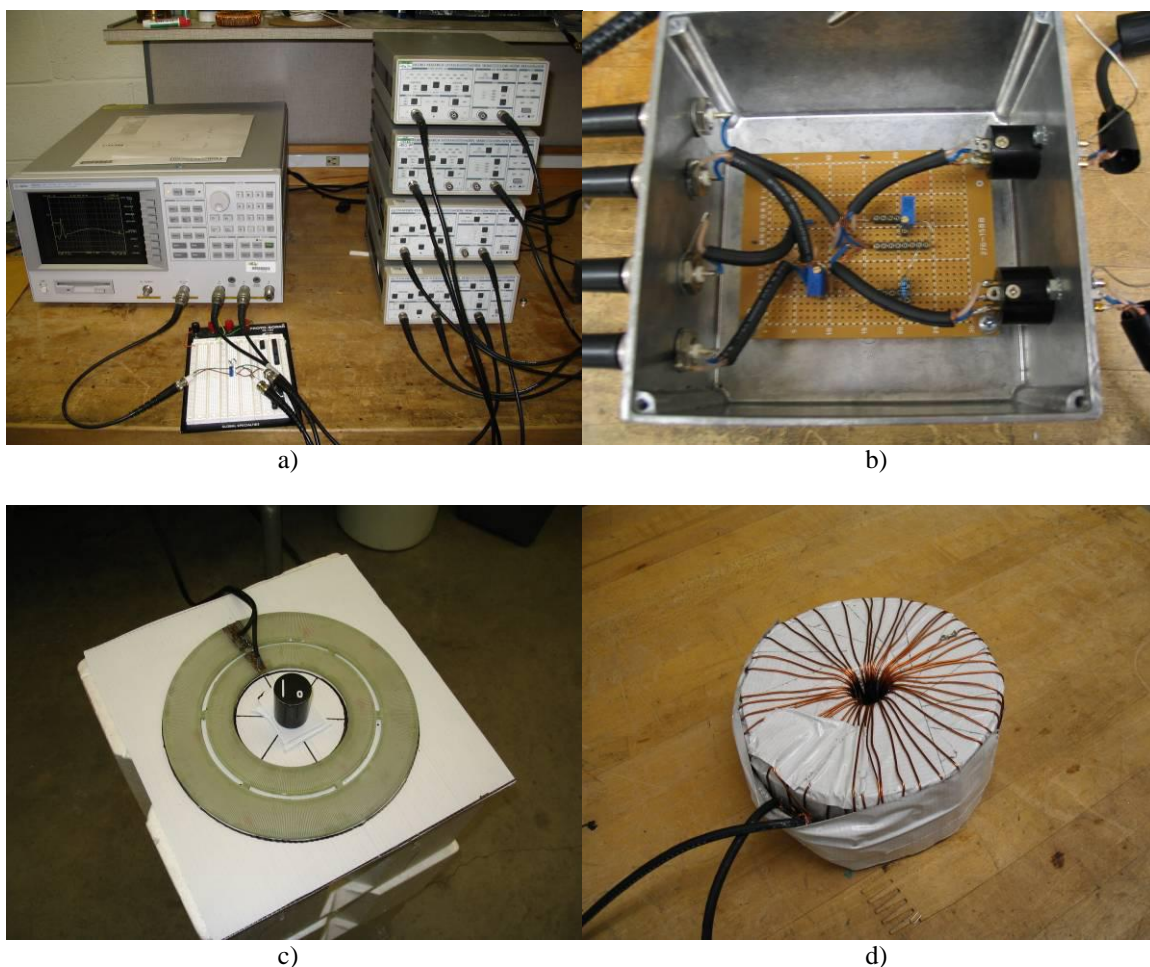


Figure 4. Experimental model to demonstrate the EMI sensor. a) Instrumentation, b) Summing and cancellation network, c) Head transformer, and d) toroidal bucking transformer.

close proximity to it. The toroid has a thickness of 1.78 inches, an inner diameter of 1.75 inches, and an outer diameter of 5.18 inches. The primary winding consists of 118 turns of 18 gauge wire, and the secondary winding consists of 46 turns of 18 gauge wire. The primary and secondary windings are shielded from each other with a metalized Mylar film that is placed between the windings and is grounded. This significantly reduces the capacitance between the primary and secondary windings.

Figure 5 is a graph of the response R from the experimental model with no target present as a function of frequency. Ideally the response will be zero with no target present. However, due to the parasitics and imperfect compensation, the response will be non zero. For the top curve, only the gain correction was used which only results in a -25 dB cancellation at 100 kHz. For the middle curve, both gain and Q correction were used resulting in better cancellation. For the bottom curve,

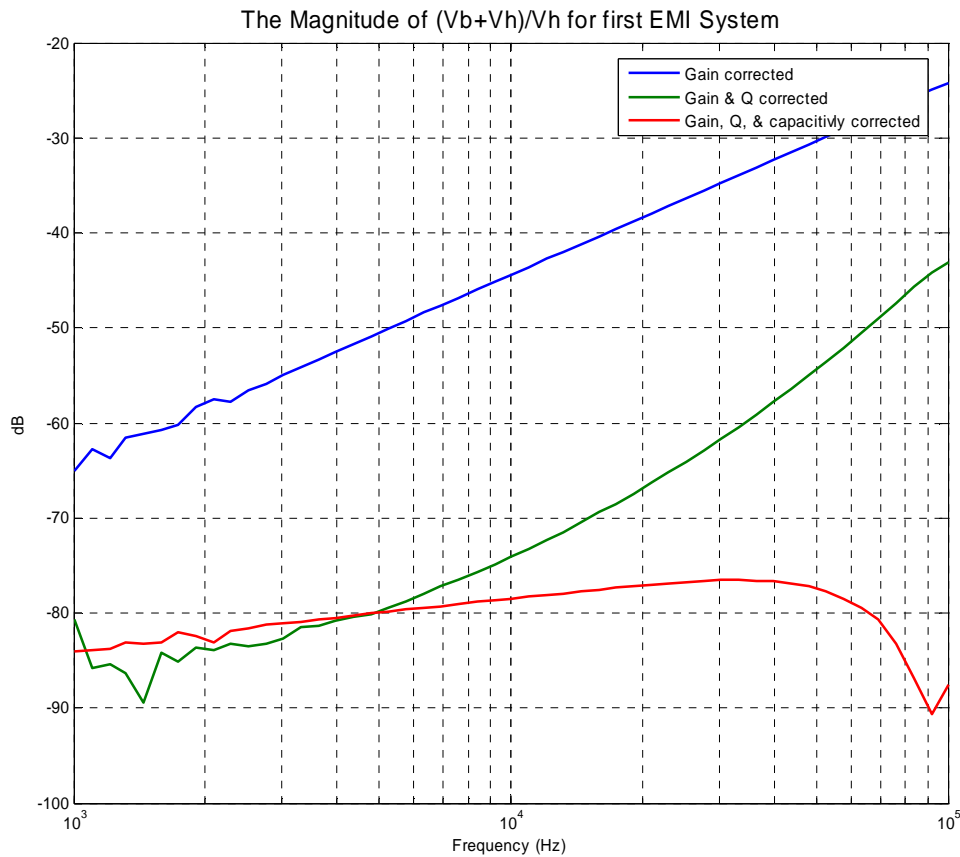


Figure 5. Response of the EMI sensor as a function of frequency.

all three corrections were used resulting in more than 75 dB of cancellation for frequencies less than 100 kHz.

Figure 6 shows the real and imaginary parts of the response of the EMI detector for an I0 target and an M14 mine as a function of frequency. To further enhance the cancellation, the response, R_o , of the sensor with no target present is measured and subtracted from the response, R_T , with the target present. A single relaxation is seen in these results with the real part of the response of the M14 mine shifted down due to its ferrous content. The noise in the data below 3 kHz is due to power line harmonics. No attempt was made to mitigate the effect of the power line harmonics in this work. The effects could be significantly mitigated by using a stronger drive current and choosing the frequencies measures more optimally so that they do not match up with power line harmonics. We believe these results are very good considering the very low drive current: $I_0 = 75$ mA.

Figure 7 shows the real and imaginary parts of the response of the EMI detector for an I0 target [6] at 6 different heights above the ground. Also, the response without a target is also shown. These

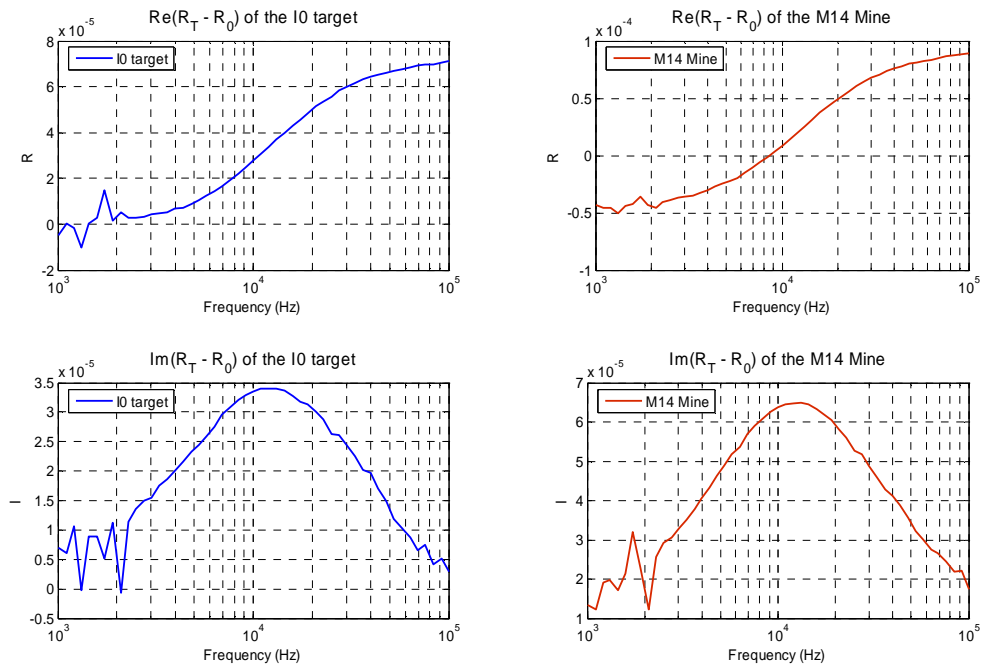


Figure 6. Real and imaginary parts of the response of an I0 target and an M14 landmine as a function of frequency.

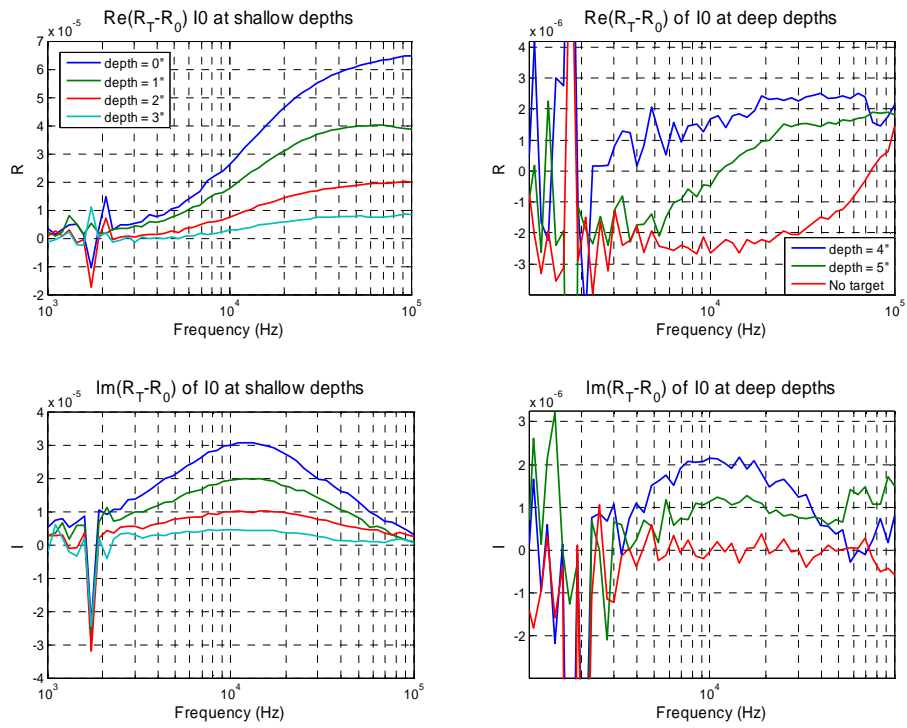


Figure 7. Response of an I0 target as function of frequency at six depths.

measurements were made with $I_0 = 75$ mA and a bandwidth of 10 Hz. The response weakens with increasing height above the sand. The effects of the target can be clearly seen at 5 inches with only a 75 mA drive current. The effects of power line harmonics remain clearly evident in the data below 3 kHz.

Conclusions

A cancellation technique using a bucking transformer and techniques for mitigating some of the parasitic effects were presented. An experimental model for the system was constructed and used to demonstrate the effectiveness of the cancellation which was more than 75 dB for frequencies less than 100 kHz. The system also demonstrated good fidelity across the entire frequency band.

Acknowledgements

This work was supported in part by the Army Research Office under Grant W911NF-04-1-0255.

References

1. P. Gao, L. Collins, P.M. Garber, N. Geng, and L. Carin, "Classification of Landmine-Like Metal Targets Using Wideband Electromagnetic Induction," *IEEE Transactions on Geoscience and Remote Sensing*, Vol. 38, No. 3, May 2000.
2. L. Collins, P. Gao, and L. Carin, "An Improved Bayesian Decision Theoretic Approach for Land Mine Detection," *IEEE Transactions on Geoscience and Remote Sensing*, Vol. 37, No. 2, March 1999.
3. G. D. Sower and S. P. Cave, "Detection and identification of mines from natural magnetic and electromagnetic resonances," in *Proc. SPIE*, Orlando, FL, 1995.
4. C. E. Baum, "Low Frequency Near-Field Magnetic Scattering from Highly, but Not Perfectly Conducting Bodies," Phillips Laboratory, *Interaction Note* 499, Nov. 1993.
5. G.T. Mallick, Jr. W.J. Carr, Jr., and R.C. Miller, "Multiple Frequency Magnetic Field Technique for Differentiating between Classes of Metal Objects," U.S. Patent 3,686,564, Aug. 22, 1972.
6. L.S. Riggs, L.T. Lowe, J.E. Mooney, T. Barnett, R. Ess, and F. Paca, "Simulants (decoys) for Low-Metallic Content Mines: Theory and Experimental Results," in *Proc. SPIE*, Vol. 3710, Orlando, FL, 1999.